Random Directional Access with and without Feedback for 5G/6G Peer-to-Peer Networks

F. Babich, F. Vatta, G. Buttazzoni, and M. Comisso
Department of Engineering and Architecture, University of Trieste, Italy,
Consorzio Nazionale Interuniveritario per le Telecomunicazioni (CNIT)
E-mail: {babich,vatta,gbuttazzoni,mcomisso}@units.it

***Abstract*— This paper theoretically analyzes the usage of directional slotted Aloha schemes for managing the peer-to-peer random access in fifth and sixth generation (5G/6G) systems. To this aim, the physical layer is modeled by accounting for interference and noise, while a Markov chain approach is developed to investigate the network behavior in the presence and in the absence of a separate feedback channel, which provides information concerning the success or not of each transmission attempt. Closed-form expressions for the coverage probability and for the transition matrices with and without feedback are derived to then evaluate the corresponding throughput. The analytical results, which are validated by independent Monte Carlo simulations, are used to estimate the impact of the antenna gain, of the burst length, and of the node density on the achievable performance, as well as to discuss the directional random access benefit/complexity tradeoff.**

***Index Terms*— Random access; directional communication; 5G/6G; peer-to-peer.**

I. Introduction

The evolutions towards the fifth-generation (5G) cellular network and then towards the space/aerial/ground sixth-generation (6G) one are targeted to the massive communication paradigm, according to which a huge number of devices share the same channel resources [1], [2]. This view concerns not only the conventional subnets of terrestrial users, sensors, and actuators, but also the fleets of unmanned aerial vehicles (UAVs), and the multi-constellation swarms of small satellites. Since the deployment of the Global System for Mobile communications (GSM), the uncoordinated management of irregular traffic flows involving stations unable to sense each other has represented a typical situation that has been dealt with the adoption of the well-established slotted Aloha (SA) protocol. This solution, which has been maintained until the present Long Term Evolution (LTE) system, is however currently under revisiting, because of the expected ultra-high node density that will characterize the 5G/6G context. In fact, several approaches have been developed in the recent years to improve the SA throughput by exploiting novel physical layer technologies, such as interference cancellation (IC) and electronically steerable antennas. Just the availability of IC-enabled receivers has stimulated the design of many evolved SA-based schemes, relying on packet repetition [3], [4], code diversity [5], non-orthogonal multiple access [6], as well as on combinations of these techniques [7], [8]. On the other hand, the compactness characteristics of the millimeter-wave (mmWave) radiating equipments [9]–[11], have invited to rediscover the application of analog beamforming to provide spatial multiplexing [12]–[14], to address the 5G initial access problem [15], [16], and to provide joint terrestrial/non-terrestrial link support to 5G/6G gateways [17], [18]. Besides, within the next-generation standards, peer-to-peer connections, in the form of device-to-device or machine-to-machine communications, are expected to play a key role for offloading the core network and reducing the end-to-end delay, even more in the presence of massive inhomogeneous traffics. This invites the adaptation of the existing random access strategies to the new challenging situations by empowering the till now implemented resource allocation algorithms.

To deal with this issue, this paper proposes a directional SA-based scheme for peer-to-peer 5G/6G subnets. The protocol is designed considering the availability and the unavailability of a separate feedback channel, having the function of enabling the source to be aware of the result of the initial access. The behavior of the developed solution is theoretically analyzed by firstly evaluating the coverage probability for the single interfered communicating pair and then adopting a Markov chain approach to model the overall network throughput. Closed-form expressions for the quantities of interest are obtained and independent Monte Carlo simulations are carried out for their validation. The derived results are finally exploited to investigate the influence of the antenna and traffic parameters on the achievable performance.

The paper is organized as follows. Section II introduces the system model. Section III presents the theoretical analysis. Section IV discusses the numerical results. Section V summarizes the most relevant conclusions.

Notation. Throughout the paper the following notation is used: $\mathbb{R}_{\geq 0}$ denotes the set of non-negative reals; $\mathbb{N}$ and $\mathbb{N}_0$ denote the sets of natural numbers with and without zero, respectively; $\mathbb{1}_{\mathbf{X}}(\mathbf{x})$ denotes the indicator function (i.e., $\mathbb{1}_{\mathbf{X}}(\mathbf{x}) = 1$ if $\mathbf{x} \in \mathbf{X}$, $\mathbb{1}_{\mathbf{X}}(\mathbf{x}) = 0$ if $\mathbf{x} \notin \mathbf{X}$); $\gamma(\cdot, x)$ denotes the lower incomplete gamma function; $(\cdot)^+$ denotes the positive part.

II. System model

Consider a pure frameless SA network with an infinite number of source-destination pairs independently communicating on a peer-to-peer basis. This network might be viewed as a set

of terrestrial users, a fleet of UAVs, a swarm of small satellites or another subnet of homogeneous devices. The arrival event consists of a burst of b consecutive packets and is modeled by a Poisson process. The time domain is subdivided into slots of identical duration, with each packet that spans one slot. According to the Poisson assumption, the probability that i bursts are generated in the network for an offered load G is given by:

$$\alpha_i(G) = \frac{G^i}{i!} \exp(-G), \quad i \in \mathbb{N}, \tag{1}$$

which also identifies the number of activated pairs. All users are assumed to adopt the same bi-dimensional modulation of order ς and the same channel encoder operating at rate ϱ. These two quantities can be jointly taken into account by considering the rate [19]:

$$R = \varrho \log_2 \varsigma, \tag{2}$$

which identifies the number of information bits carried by each transmission, symbol, or channel use. Concerning the burst length b (in packets), it is the realization of a geometrically distributed random variable (r.v.) $\mathcal{B}$ having probability mass function (pmf):

$$f_{\mathcal{B}}(b) = \frac{1}{\Lambda}\left(1 - \frac{1}{\Lambda}\right)^{b-1}, \quad b \in \mathbb{N}_0, \tag{3}$$

where Λ is the average burst length. The overall reception is modeled considering two stages: the initial access and the burst acquisition. The first one is carried out at the beginning of the reception using the available analog antenna system in omnidirectional operating mode to make each source and the corresponding destination aware of the intended communication. If this first stage is successful, at the end of it the destination has generated a directional pattern with the main lobe steered towards its source. The second stage exploits this pattern to receive the remaining packets of the burst in directional operating mode, while the source maintains the omnidirectional transmission. Retransmissions are not allowed, thus each packet, once transmitted, is discarded from the queue of the source. Therefore, from the point of view of a generic target pair, the receiving gain is equal to unity for the initial access. For the burst acquisition after a successful first stage, instead, it is assumed equal to the maximum gain $\Theta(\geq 1)$ towards a desired source and equal to the backlobe gain $\theta(\leq 1)$ towards an undesired one. Hence, when $n \in \mathbb{N}_0$ pairs are active, the power received by the target destination from a generic l-th source (desired or undesired) may be compactly described by the r.v.:

$$P_l = \chi \Psi_l g_l, \;\; l = 1, ..., n, \tag{4}$$

where χ is a parameter accounting for the constant quantities (transmission power, carrier wavelength, antenna heights, ...), Ψ_l is a r.v. jointly accounting for the statistical phenomena that characterize the propagation channel between the l-th source and the target destination (path-loss, fast- and mid-scale fading, ...), while:

$$g_l = \begin{cases} \Theta & l = 1 \\ \theta & l = 2, ..., n \end{cases}. \tag{5}$$

Without loss of generality, the index $l = 1$ is used to identify the target source. Note that (4) includes the powers referred to both stages, since the initial access simply corresponds to $\Theta = \theta = 1$. The n r.v.s $\Psi_1, ..., \Psi_n$ are assumed independent and identically distributed (i.i.d.) unit-mean exponential, thus they are described by the probability density function (pdf):

$$f_{\Psi_l}(\psi_l) = \exp(-\psi_l) \mathbb{1}_{\mathbb{R}_{\geq 0}}(\psi_l), \;\; l = 1, ..., n. \tag{6}$$

Beside the interference deriving from the undesired sources, the destination is subject to noise, whose power can be evaluated as [20]:

$$\sigma^2_{\mathcal{N}} = \zeta \cdot B_W \cdot \mathcal{F}_{\mathcal{N}}, \tag{7}$$

where $\zeta \cong 3.98 \cdot 10^{-21}$ W/Hz is the noise spectral density, while B_W and $\mathcal{F}_{\mathcal{N}}$ are, respectively, the bandwidth and the noise figure of the receiver.

III. Analysis

To theoretically analyze the performance of the introduced directional SA scheme, consider first the coverage probability, namely the probability that the signal to interference plus noise ratio (SINR) experienced by the target destination be larger or equal to a threshold υ, which is related to the packet length, the modulation scheme, the channel encoder, and the selected packet error rate. This quantity, which models the single-packet success for the single-pair interfered communication, can be estimated according to the following proposition.

Proposition 1 (Coverage probability): Let P_l be defined by (4) and Ψ_l be distributed according to (6). Then, the coverage probability for the burst acquisition stage when $n \in \mathbb{N}_0$ communications are active can be evaluated as:

$$\eta_n^{\mathrm{D}} = \frac{\Theta^{n-1}}{(\Theta + \theta\upsilon)^{n-1}} \exp\left(-\frac{\sigma^2_{\mathcal{N}}\upsilon}{\chi\Theta}\right). \tag{8}$$

Proof: See Appendix A-A. □

Note that (8) includes also the noise-limited case ($n = 1$), in which no interfering pairs are active, and, similarly to (4), can provide, for $\Theta = \theta = 1$, the coverage probability for the initial access stage as:

$$\eta_n^{\mathrm{O}} = \frac{1}{(1 + \upsilon)^{n-1}} \exp\left(-\frac{\sigma^2_{\mathcal{N}}\upsilon}{\chi}\right). \tag{9}$$

To maintain the mathematical tractability of the analysis and simplify the reproducibility of the results, just Rayleigh fading and noise have been considered in the propagation environment, but, if required, further statistical phenomena may be readily added to the channel model.

Once the coverage probabilities are available, one can focus on the estimation of the throughput by adopting a Markov chain to model the evolution of the network. Within this task, two situations are considered: a first one in which the success

of the initial access is communicated to the target source by the target destination through a separate feedback channel, and a second one in which, instead, this channel is absent.

Consider first the presence of the feedback mechanism. The information provided by this channel enables the source to decide whether to transmit the rest of the burst or not. More precisely, if the first packet of the burst has been correctly received, the initial access has been successful and the source is aware of being allowed to send the remaining packets of the same burst. Otherwise, the burst transmission is aborted. The evolution of this system may be modeled by a two-dimensional Markov chain. In each slot, the generic state (i, j) accounts for the number i of sources that have successfully completed the initial access stage and for the number j of sources involved in the acquisition stage. The transition matrix modeling this situation can be built in agreement with the following proposition.

Proposition 2 (Transition matrix with feedback channel): Let the burst arrival and the burst length be distributed according to (1) and (3), respectively. Then, the generic element of the four-dimensional matrix describing the transition from the previous state (i', j') to the current one (i, j) in the presence of the feedback channel can be expressed, for $i', j', i, j \in \mathbb{N}$, as:

$$T_{i'j'}^{ij} = \alpha_i(G)\,\frac{(\Lambda-1)^j}{\Lambda^{j'}}\left[1-\left(1-\frac{1}{\Lambda}\right)\eta_{i'}^{\mathrm{O}}\eta_{j'}^{\mathrm{D}}\right]^{i'} \sum_{k=(j-j')^+}^{\min(i',j)} \frac{\binom{i'}{k}\binom{j'}{j-k}}{\left[1-\Lambda\left(1-\frac{1}{\eta_{i'}^{\mathrm{O}}\,\eta_{j'}^{\mathrm{D}}}\right)\right]^{k}}. \tag{10}$$

where the values $\eta_0^{\mathrm{O}} = \eta_0^{\mathrm{D}} = 1$ are defined for mathematical purposes.

Proof: See Appendix A-B. □

Within the summation in (10), which accounts for the capture effects as well as for the length of the burst in the first and second stage, the index k denotes the number of successful initial accesses corresponding to sources that have further packets to transmit in their burst. Once the transition matrix is characterized, the steady-state probabilities $\pi_{i,j}$ $(i, j \in \mathbb{N})$ may be determined through iterative techniques [21], from which the throughput and the actual load can be evaluated, respectively, as:

$$S = R \sum_{i,j\in\mathbb{N}} \pi_{i,j}\left(i\eta_i^{\mathrm{O}} + j\eta_j^{\mathrm{D}}\right), \tag{11}$$

and:

$$G_{\mathrm{e}} = \sum_{i,j\in\mathbb{N}} \pi_{i,j}\,(i+j). \tag{12}$$

Observe that, in (11), the throughput, which is obtained by multiplying the rate with the average successfully transmitted packets per slot, is expressed in information bits per transmission. This allows one to compare systems operating with different rates and, as a consequence, with different thresholds. Moreover, in (12), G_{e} takes into account the sole packets that are actually transmitted after a positive feedback and is hence not directly proportional to the total offered load G in (1).

Consider now the case without feedback. In this situation, the source has no information concerning the result of the initial access. Hence, the burst acquisition begins regardless of the success or not of the first stage. More precisely, the source anyway keeps on transmitting the rest of the burst to its destination, which adopts a directional pattern if the first stage has been successful, and an omnidirectional one otherwise. The description of this second system requires a three-dimensional Markov chain, where now, in each slot, the generic state $(i_{\mathrm{n}}, i_{\mathrm{o}}, j)$ accounts for the number i_{n} of sources that have successfully completed the initial access stage, for the number i_{o} of sources that have failed the initial access stage (but will anyway go on transmitting the rest of their bursts), and for the number j of sources involved in the acquisition stage. The transition matrix characterizing this scenario can be determined through the following proposition.

Proposition 3 (Transition matrix without feedback channel): Let the burst arrival and the burst length be distributed according to (1) and (3), respectively. Then, the generic element of the six-dimensional matrix describing the transition from the previous state $(i'_{\mathrm{n}}, i'_{\mathrm{o}}, j')$ to the current one $(i_{\mathrm{n}}, i_{\mathrm{o}}, j)$ in the absence of the feedback channel can be expressed, for $i'_{\mathrm{n}}, i'_{\mathrm{o}}, j', i_{\mathrm{n}}, i_{\mathrm{o}}, j \in \mathbb{N}$, as:

$$T_{i'_{\mathrm{o}}i'_{\mathrm{n}}j'}^{i_{\mathrm{o}}i_{\mathrm{n}}j} = \alpha_{i_{\mathrm{n}}}(\lambda)\,\frac{(\Lambda-1)^{i_{\mathrm{o}}+j}}{\Lambda^{i'_{\mathrm{o}}+i'_{\mathrm{n}}+j'}} \sum_{k=(j-j')^+}^{\min(i'_{\mathrm{n}},j)} \binom{i'_{\mathrm{n}}}{k}\binom{j'}{j-k}\left(\eta_{i'_{\mathrm{o}}+i'_{\mathrm{n}}}^{\mathrm{O}}\eta_{j'}^{\mathrm{D}}\right)^k \left[\sum_{q=(i_{\mathrm{o}}-i'_{\mathrm{o}})^+}^{\min(i'_{\mathrm{o}},i'_{\mathrm{n}}-k)} \binom{i'_{\mathrm{n}}-k}{q}\binom{i'_{\mathrm{o}}}{i_{\mathrm{o}}-q}\left(1-\eta_{i'_{\mathrm{o}}+i'_{\mathrm{n}}}^{\mathrm{O}}\eta_{j'}^{\mathrm{D}}\right)^q\right]. \tag{13}$$

Proof: See Appendix A-C. □

Within the summation in (13), the index k maintains the same meaning as in (10), while the index q denotes the number of successful burst acquisitions corresponding to sources that have completed their transmission. Besides, similarly to the previous case, the availability of the transition matrix enables to iteratively derive the corresponding steady-state probabilities $\pi_{i_{\mathrm{n}},i_{\mathrm{o}},j}$ $(i_{\mathrm{n}}, i_{\mathrm{o}}, j \in \mathbb{N})$ [21], from which the throughput and the actual load can be now estimated, respectively, as:

$$S = R \sum_{i_{\mathrm{n}},i_{\mathrm{o}},j\in\mathbb{N}} \pi_{i_{\mathrm{n}},i_{\mathrm{o}},j}\left[(i_{\mathrm{n}}+i_{\mathrm{o}})\,\eta_{i_{\mathrm{n}}+i_{\mathrm{o}}}^{\mathrm{O}} + j\eta_j^{\mathrm{D}}\right], \tag{14}$$

and:

$$G_{\mathrm{e}} = G\Lambda, \tag{15}$$

where the absence of feedback implies that G_{e} is directly proportional to the total offered load, since now the source accomplishes the transmission of its burst regardless of the success or not of the initial access. These latter formulas and

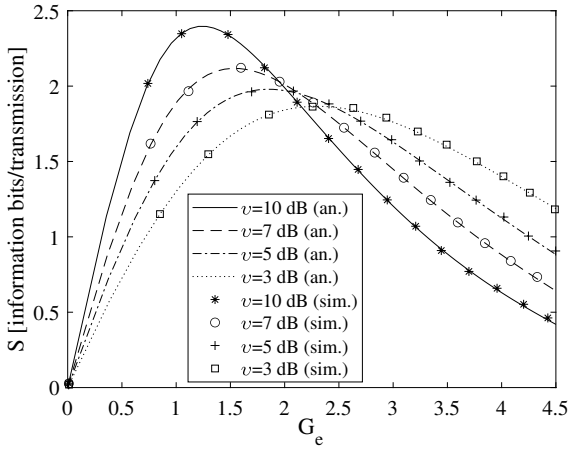

Fig. 1. Throughput as a function of the actual load for the proposed scheme with feedback for $\Lambda = 10$, $\Theta = 5$ dB, $\theta = -5$ dB, and different thresholds.

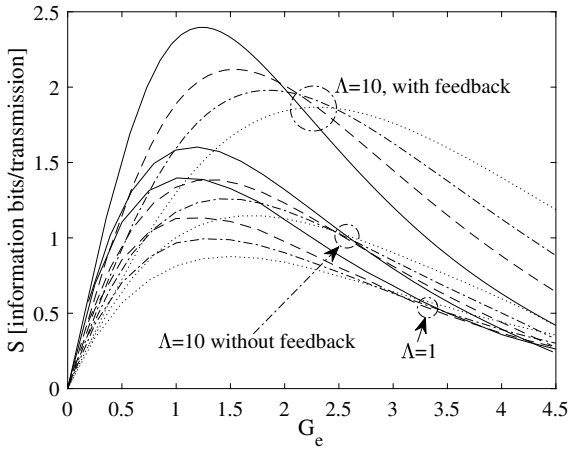

Fig. 2. Throughput as a function of the actual load for the basic SA ($\Lambda = 1$, $\Theta = \theta = 0$ dB) and for the proposed schemes with and without feedback ($\Lambda = 10$, $\Theta = 5$ dB, $\theta = -5$ dB) considering different thresholds: $\upsilon = 10$ dB (solid), $\upsilon = 7$ dB (dashed), $\upsilon = 5$ dB (dash-dotted), $\upsilon = 3$ dB (dotted).

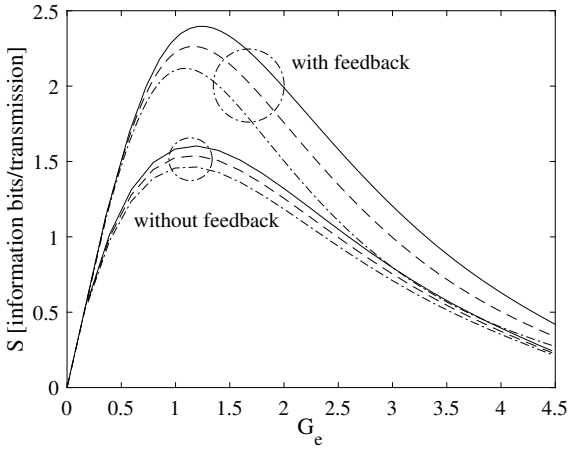

Fig. 3. Throughput as a function of the actual load for the proposed schemes with and without feedback for $\Lambda = 10$, $\upsilon = 10$ dB, $\theta = -5$ dB, and different maximum gains: $\Theta = 10$ dB (solid), $\Theta = 8$ dB (dashed), $\Theta = 5$ dB (dash-dotted).

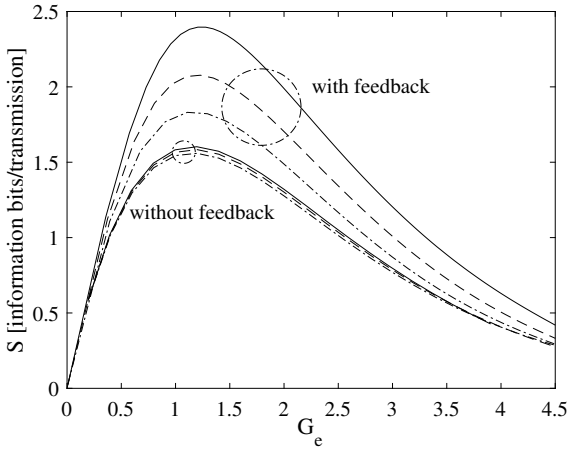

Fig. 4. Throughput as a function of the actual load for the proposed schemes with and without feedback for $\upsilon = 10$ dB, $\Theta = 5$ dB, $\theta = -5$ dB, and different average burst lengths: $\Lambda = 10$ (solid), $\Lambda = 5$ (dashed), $\Lambda = 3$ (dash-dotted).

those provided in (10)-(12) for the feedback case show that the performance of the presented directional SA system may be usefully characterized through analytical expressions relying on closed-form coverage probability estimations.

IV. Results

This section presents the results derived from the proposed framework, which are obtained assuming a receiver characterized by a bandwidth $B_W = 1$ GHz and a noise figure $\mathcal{F}_{\mathcal{N}} = 10$ dB. Besides, all summations and transition matrices in (10)-(14) are evaluated by considering state indexes not larger than 12 for limiting the computational burden required to model the network evolution in the contention states.

The first set of curves is illustrated in Fig. 1, which reports the throughput as a function of the actual load for $\Lambda = 10$, $\Theta = 5$ dB, $\theta = -5$ dB, and different thresholds for the proposed scheme in the presence of feedback. To check the accuracy of the analytical values (identified by lines), Monte Carlo simulations (identified by markers) are carried out. The figure puts into evidence that the higher the SINR threshold, the higher the maximum achievable throughput. This behavior, which is emphasized by the Rayleigh fading statistic, may be explained observing that a higher υ value implies a higher modulation order, thus leading, according to (2), to a higher rate and, in turn, to more information bits carried by each successful communication. Concerning the accuracy of the analysis, one may notice that the adopted limitation of the implemented formulas to state indexes not larger than 12 does not affect the performance. A really satisfactory matching between theoretical and simulated curves may be in fact observed. Since this matching has been confirmed also for the subsequent results, in the sequel the simulations will be no more reported to maintain the readability of the figures.

A second set of results is shown in Fig. 2, which compares, for the same thresholds used in Fig. 1, the performance of the feedback and no feedback scenarios, modeled considering $\Lambda = 10$, $\Theta = 5$ dB, and $\theta = -5$ dB, with that of the typical

SA system with capture, modeled considering $\Lambda = 1$ and $\Theta = \theta = 0$ dB. This latter system substantially involves the sole initial access realized in omnidirectional operating mode. By taking the SA curves as references, the comparison reveals the expected significant throughput improvement achievable when the feedback channel is available, while just a moderate increase is observable in the opposite case. This difference is mainly due to the considerably lower coverage probability of the initial access with respect to that of the acquisition stage, which makes the feedback information fundamental to avoid waste of resources and useless interference due to unsuccessful burst transmissions.

The third set of results, reported in Fig. 3 and obtained for $\Lambda = 10$, $\upsilon = 10$ dB, and $\theta = -5$ dB, focuses on the impact of the maximum antenna gain. With respect to the increase of this parameter, the main benefits are achieved by the feedback-based scheme, which is more sensitive to the SINR improvements during the acquisition stage as compared to the no feedback one, whose performance is decreased by the waste of resources due to the useless and unsuccessful omnidirectional receptions. This difference between the two cases is further emphasized when different average burst lengths are considered. In fact, Fig. 4, which is derived for $\upsilon = 10$ dB, $\Theta = 5$ dB, and $\theta = -5$ dB, shows the negligible impact of Λ on the throughput of the no feedback scheme, since this solution is substantially insensitive to the burst length after an unsuccessful initial access. Conversely, the feedback-based scheme is able to properly exploit the Λ increase, since this event corresponds to a longer acquisition stage achieved after an acknowledged successful initial access.

In general, from the above discussed figures, one may infer that, by adopting suitable values for the antenna gains, the burst length, and the SINR threshold, the throughput improvement with respect to the SA protocol may be significant when a basic feedback mechanism is available. Furthermore, the not high Θ and υ values adopted to obtain the presented results suggest that simple antenna systems and low-order modulations may be sufficient to achieve a satisfactory behavior, hence revealing a good tradeoff between performance gain and complexity increase.

V. Conclusions

A theoretical model has been developed to evaluate the benefits deriving from the adoption of directional receptions in SA schemes for managing the peer-to-peer random access procedure in forthcoming 5G/6G systems. Analytical expressions, validated through independent Monte Carlo simulations, for the coverage probability and for the Markov chain transition matrices have been conceived to estimate the overall network throughput for the feedback and no feedback cases. The results have shown that considerable benefits are already obtained implementing in the SA protocol a basic feedback mechanism combined with simple radiating systems and not sophisticated code-modulation pairs. Further improvements may be achieved considering longer burst sequences and larger antenna gains. This second aspect is currently under investigation together with a more detailed characterization of the propagation environment. Current research efforts are in fact devoted to the introduction of directional transmissions during the acquisition stage and to the derivation of manageable closed-form expressions for the coverage probability in the millimeter-wave channel at the different 6G atmospheric layers (terrestrial, aerial, spatial).

Appendix A

A. Proof of Proposition 1

As a first step, by using (6) and the scaling rule of r.v.s [22], calculate the pdf of P_l in (4) as:

$$f_{P_l}(p_l) = \frac{1}{\chi g_l} \exp\left(-\frac{p_l}{\chi g_l}\right) \mathbb{1}_{\mathbb{R}_{\geq 0}}(p_l), \;\; l = 1, ..., n. \quad (16)$$

Define now the r.v.:

$$U = \sum_{l=2}^{n} P_l + \sigma_{\mathcal{N}}^2, \quad (17)$$

representing the undesired power given by sum of interference and noise. Since, by (5), $g_l = \theta$ for $l = 2, ...n$, the r.v.s $P_2, ...P_n$ are i.i.d. exponential, and hence U follows a translated Erlang distribution [23], whose cumulative distribution function (cdf) may be written as:

$$F_U^n(u) = \frac{1}{(n-2)!} \gamma\left(n-1, \frac{u-\sigma_{\mathcal{N}}^2}{\chi\theta}\right) \mathbb{1}_{[\sigma_{\mathcal{N}}^2, +\infty)}(u). \quad (18)$$

The r.v. representing the SINR referred to the target communication ($l = 1$) can now be defined as:

$$\Upsilon = \frac{P_1}{U}, \quad (19)$$

whose cdf can be evaluated from (16) and (18) by applying the ratio distribution [22], as:

$$\begin{aligned} F_\Upsilon^n(\upsilon) &= \int_0^{+\infty} f_{P_1}(p_1) F_U^n\left(\frac{p_1}{\upsilon}\right) \mathrm{d}p_1 \\ &= \frac{1}{\chi\Theta(n-2)!} \int_{\upsilon\sigma_{\mathcal{N}}^2}^{+\infty} \left\{ \gamma\left[n-1, \frac{1}{\chi\theta}\left(\frac{p_1}{\upsilon} - \sigma_{\mathcal{N}}^2\right)\right] \right. \\ &\qquad \left. \exp\left(-\frac{p_1}{\chi\theta}\right) \right\} \mathrm{d}p_1 \\ &= \left[1 - \frac{\Theta^{n-1}}{(\Theta + \theta\upsilon)^{n-1}} \exp\left(-\frac{\sigma_{\mathcal{N}}^2 \upsilon}{\chi\Theta}\right)\right] \mathbb{1}_{\mathbb{R}_{\geq 0}}(\upsilon). \quad (20) \end{aligned}$$

By remembering that the coverage probability is the complementary cdf of the SINR and has meaning for $\upsilon \geq 0$, one immediately obtains (8).

B. Proof of Proposition 2

The transition probability from the previous state (i', j') to the current one (i, j) for $i', j', i, j \in \mathbb{N}$ in the presence of feedback is given by:

$$T_{i'j'}^{ij} = \alpha_i(G) \sum_{k=(j-j')^+}^{\min(i',j)} \sum_{q=0}^{i'-k} \left[t_{k+q,k} \left(\eta_{i'}^{\mathrm{O}} \eta_{j'}^{\mathrm{D}}\right)\right.$$

$$\cdot\, t_{i',i'-k-q}\left(\frac{1}{\Lambda}\right)\cdot t_{j',j'-j+k}\left(\frac{1}{\Lambda}\right)\Bigg], \qquad (21)$$

where:

$$t_{h,l}(x)=\binom{h}{l}x^l(1-x)^{h-l}, \qquad (22)$$

denotes the binomial function, holding for $h\geq l$. Besides, in (21), the first binomial function accounts for the capture effect, while the second and the third one account for the length of the burst in the access and acquisition stage, respectively. By substituting (22) in (21), exploiting the row-symmetry property of the binomial coefficient, and then manipulating, (21) itself can be rewritten as:

$$\begin{aligned}T^{ij}_{i'j'}&=\alpha_i(G)\,\frac{(\Lambda-1)^j}{\Lambda^{i'+j'}}\sum_{k=(j-j')^+}^{\min(i',j)}\binom{j'}{j-k}\left(\eta^{\mathrm{O}}_{i'}\eta^{\mathrm{D}}_{j'}\right)^k\\&\quad\left\{\sum_{q=0}^{i'-k}\binom{i'}{k+q}\binom{k+q}{k}\left[(\Lambda-1)\left(1-\eta^{\mathrm{O}}_{i'}\eta^{\mathrm{D}}_{j'}\right)\right]^q\right\}\\&=\alpha_i(G)\,\frac{(\Lambda-1)^j}{\Lambda^{i'+j'}}\sum_{k=(j-j')^+}^{\min(i',j)}\binom{i'}{k}\binom{j'}{j-k}\left(\eta^{\mathrm{O}}_{i'}\eta^{\mathrm{D}}_{j'}\right)^k\\&\quad\left[1+(\Lambda-1)\left(1-\eta^{\mathrm{O}}_{i'}\eta^{\mathrm{D}}_{j'}\right)\right]^{i'-k}, \qquad (23)\end{aligned}$$

where the summation on the index q is solved by applying the subset-of-a-subset property and then the binomial theorem. Now, by reordering the terms and performing few algebra, one finally obtains (10).

C. Proof of Proposition 3

The transition probability from the previous state $(i'_{\mathrm{n}},i'_{\mathrm{o}},j')$ to the current one $(i_{\mathrm{n}},i_{\mathrm{o}},j)$ for $i'_{\mathrm{n}},i'_{\mathrm{o}},j',i_{\mathrm{n}},i_{\mathrm{o}},j\in\mathbb{N}$ in the absence of feedback is given by:

$$\begin{aligned}T^{i_{\mathrm{o}}i_{\mathrm{n}}j}_{i'_{\mathrm{o}}i'_{\mathrm{n}}j'}&=\alpha_{i_{\mathrm{n}}}(\lambda)\sum_{k=(j-j')^+}^{\min(i'_{\mathrm{n}},j)}\sum_{q=(i_{\mathrm{o}}-i'_{\mathrm{o}})^+}^{\min(i'_{\mathrm{o}},i'_{\mathrm{n}}-k)}\Bigg[t_{k+q,k}\left(\eta^{\mathrm{O}}_{i'_{\mathrm{o}}+i'_{\mathrm{n}}}\eta^{\mathrm{D}}_{j'}\right)\\&\cdot t_{i'_{\mathrm{o}},i'_{\mathrm{o}}-i_{\mathrm{o}}+q}\left(\frac{1}{\Lambda}\right)\cdot t_{i'_{\mathrm{n}},i'_{\mathrm{n}}-k-q}\left(\frac{1}{\Lambda}\right)\cdot t_{j',j'-j+k}\left(\frac{1}{\Lambda}\right)\Bigg]. \qquad (24)\end{aligned}$$

Similarly to the previous proof, the use of (22) and of the binomial row-symmetry property enable to manipulate (24) so as to derive:

$$\begin{aligned}T^{i_{\mathrm{o}}i_{\mathrm{n}}j}_{i'_{\mathrm{o}}i'_{\mathrm{n}}j'}&=\alpha_{i_{\mathrm{n}}}(\lambda)\,\frac{(\Lambda-1)^{i_{\mathrm{o}}+j}}{\Lambda^{i'_{\mathrm{o}}+i'_{\mathrm{n}}+j'}}\sum_{k=(j-j')^+}^{\min(i'_{\mathrm{n}},j)}\binom{j'}{j-k}\left(\eta^{\mathrm{O}}_{i'_{\mathrm{o}}+i'_{\mathrm{n}}}\eta^{\mathrm{D}}_{j'}\right)^k\\&\left[\sum_{q=(i_{\mathrm{o}}-i'_{\mathrm{o}})^+}^{\min(i'_{\mathrm{o}},i'_{\mathrm{n}}-k)}\binom{i'_{\mathrm{n}}}{k+q}\binom{k+q}{k}\binom{i'_{\mathrm{o}}}{i_{\mathrm{o}}-q}\left(1-\eta^{\mathrm{O}}_{i'_{\mathrm{o}}+i'_{\mathrm{n}}}\eta^{\mathrm{D}}_{j'}\right)^q\right], \qquad (25)\end{aligned}$$

from which, by applying the subset-of-a-subset property to the first two binomial coefficients present in the second summation, one immediately obtains (13).

REFERENCES

[1] J.G. Andrews, S. Buzzi, W. Choi, S.V. Hanly, A. Lozano, A.C.K. Soong, and J.C. Zhang, "What will 5G be?" *IEEE J. Sel. Areas Commun.*, vol. 32, no. 6, pp. 1065–1082, June 2014.

[2] M. Giordani and M. Zorzi, "Non-terrestrial networks in the 6G era: Challenges and opportunities," *IEEE Netw.*, vol. 35, no. 2, pp. 244–251, Mar./Apr. 2019.

[3] E. Casini, R. De Gaudenzi, and O. del Río Herrero, "Contention resolution diversity slotted ALOHA (CRDSA): An enhanced random access scheme for satellite access packet networks," *IEEE Trans. Wireless Commun.*, vol. 6, no. 4, pp. 1408–1419, Apr. 2007.

[4] G. Liva, "Graph-based analysis and optimization of contention resolution diversity slotted ALOHA," *IEEE Trans. Commun.*, vol. 59, no. 2, pp. 477–487, Feb. 2011.

[5] E. Paolini, G. Liva, and M. Chiani, "Coded slotted ALOHA: A graph-based method for uncoordinated multiple access," *IEEE Trans. Inf. Theory*, vol. 61, no. 12, pp. 6815–6832, Dec. 2015.

[6] J.-B. Seo, B.C. Jung, and H. Jin, "Nonorthogonal random access for 5G mobile communication systems," *IEEE Trans. Veh. Technol.*, vol. 67, no. 38, pp. 7867–7871, Aug. 2018.

[7] S. Alvi, S. Durrani, and X. Zhou, "Enhancing CRDSA with transmit power diversity for machine-type communication," *IEEE Trans. Veh. Technol.*, vol. 67, no. 8, pp. 7790–7794, Aug. 2018.

[8] X. Shao, Z. Sun, M. Yang, S. Gu, and Q. Guo, "NOMA-based irregular repetition slotted ALOHA for satellite networks," *IEEE Commun. Lett.*, vol. 23, no. 4, pp. 624–627, Apr. 2019.

[9] M. Comisso, "On the use of dimension and lacunarity for comparing the resonant behavior of convoluted wire antennas," *Progr. Electromag. Res., PIER 96*, pp. 361–376, 2009.

[10] X. Shen, Y. Liu, L. Zhao, G.-L. Huang, X. Shi, and Q. Huang, "A miniaturized microstrip antenna array at 5G millimeter-wave band," *IEEE Antennas Wireless Propag. Lett.*, vol. 18, no. 8, pp. 1671–1675, Aug. 2019.

[11] Y.J. Guo, M. Ansari, R.W. Ziolkowski, and N.J.G. Fonseca, "Quasi-optical multi-beam antenna technologies for B5G and 6G mmWave and THz networks: A review," *IEEE Open J. Antennas Propag.*, vol. 2, pp. 807–830, June 2021.

[12] X. Yu, J. Zhang, M. Haenggi, and K.B. Letaief, "Coverage analysis for millimeter wave networks: The impact of directional antenna arrays," *IEEE J. Sel. Areas Commun.*, vol. 35, no. 7, pp. 1498–1512, July 2017.

[13] F. Babich and M. Comisso, "Multi-packet communication in heterogeneous wireless networks adopting spatial reuse: Capture analysis," *IEEE Trans. Wireless Commun.*, vol. 12, no. 10, pp. 5346–5359, Oct. 2013.

[14] D. Pinchera, M.D. Migliore, and F. Schettino, "Optimizing antenna arrays for spatial multiplexing: Towards 6G systems," *IEEE Access*, vol. 9, pp. 53 276–53 291, Mar. 2021.

[15] C.N. Barati, S.A. Hosseini, M. Mezzavilla, T. Korakis, S.S. Panwar, S. Rangaan, and M. Zorzi, "Initial access millimeter wave cellular systems," *IEEE Trans. Wireless Commun.*, vol. 15, no. 12, pp. 7926–7940, Dec. 2016.

[16] W. Attaoui, K. Bouraqia, and E. Sabir, "Initial access and beam alignment for mmWave and terahertz communications," *IEEE Access*, vol. 10, pp. 35 363–35 397, Mar. 2022.

[17] M. Vaezi, A. Azari, S.R. Khosravirad, M. Shirvanimoghaddam, M. Mahdi Azari, D. Chasaki, and P. Popovski, "Cellular, wide-area, and non-terrestrial IoT: A survey on 5G advances and the road towards 6G," *IEEE Commun. Surv. Tut.*, vol. 24, no. 2, pp. 1117–1174, Apr.-June 2022.

[18] I.I. Ioannou, C. Christophorou, V. Vassiliou, M. Lestas, and A. Pitsillides, "Dynamic D2D communication in 5G/6G using a distributed AI framework," *IEEE Access*, vol. 10, pp. 62 772–62 799, June 2022.

[19] F. Babich and M. Comisso, "Impact of segmentation and capture on slotted Aloha systems exploiting interference cancellation," *IEEE Trans. Veh. Technol.*, vol. 68, no. 3, pp. 2878–2892, Mar. 2019.

[20] M. Di Renzo, "Stochastic geometry modeling and analysis of multi-tier millimeter wave cellular networks," *IEEE Trans. Wireless Commun.*, vol. 14, no. 9, pp. 5038–5057, Sep. 2015.

[21] F. Babich and M. Comisso, "Theoretical analysis of asynchronous multi-packet reception in 802.11 networks," *IEEE Trans. Commun.*, vol. 58, no. 6, pp. 1782–1794, June 2010.

[22] R.D. Yates and D.J. Goodman, *Probability and Stochastic Processes*. Ed. New York: Wiley, 1999.

[23] V. Krishnan, *Probability and Random Processes*. Ed. New York: Wiley, 2006.